Video Packet Scheduling With Stochastic QoS for Cognitive Heterogeneous Networks

Lei Xu, *Member, IEEE*, Arumugam Nallanathan, *Fellow, IEEE*, and Yuwang Yang

***Abstract*—In this paper, a video framework with stochastic quality of service (QoS) is proposed for cognitive heterogeneous networks based on internetwork cooperation. The video packet scheduling is subject to constraints in the available energy at each call for secondary mobile terminal (MT), the time varying channel state information (CSI) at different interfaces, the total interference power, the target call duration, and the video characteristics. The objective function maximizes the minimum lower bound of video quality. In order to solve the above video packet scheduling problem with stochastic QoS guarantee, a video packet scheduling scheme based on forward-auction theory is proposed. Then, the cumulative distribution function (CDF) for video quality is analyzed. Finally, the power allocation scheme to maximize the minimization lower bound of video quality among different secondary MTs is presented. Simulation results demonstrate that the proposed video packet scheduling scheme with stochastic QoS requirement improves the video quality for secondary MT significantly.**

***Index Terms*—Auction theory, cognitive heterogeneous networks, internetwork cooperation, stochastic quality of service (QoS), video packet scheduling.**

I. Introduction

WIRELESS communication technologies in the fifth-generation (5G) mobile communication systems are growing rapidly [1], [2], which lead to radio spectrum resources being more scarce. Cognitive radio is proposed to improve the spectrum utilization by allowing unlicensed mobile terminals (MTs) to use licensed frequency band resource [3]–[7]. Additionally, several international standardization organizations make some drafts for cognitive radio technology, e.g., 802.11 af, 802.19 TG 1, and LTE-U [8]–[11]. At the same time, video traffic has become very popular in mobile Internet. However, compared to traditional voice and data traffic, video traffic is still a challenging problem for cognitive wireless networks. This is because the spectral resource in cognitive wireless network is sparse and video traffic needs to consume more radio resource. Hence, different network resources at cognitive heterogeneous networks need to be aggregated to support the video traffic at secondary MT [12].

In order to guarantee the video quality requirement, video packet scheduling technology is very important. So far, the video packet scheduling algorithms at wireless networks are divided into two categories [13]–[24]. The first category is the video packet scheduling algorithms at homogeneous wireless network [13]–[22], where the optimization objectives are to maximize the video quality or achieve the higher energy efficiency. The second category is the video packet scheduling algorithms for heterogeneous wireless networks [23], [24], where the packet scheduler determines which video packet is assigned to which radio interface at each MT based on channel state information (CSI),[1] the available bandwidth resource and the video traffic characteristics.

At the homogeneous wireless network, an energy-efficient video packet scheduling policy is proposed for wireless local area networks [13]. In [14], an energy-efficient video packet scheduling algorithm to improve throughput is proposed over WiMAX for video streaming traffic. On the other hand, a joint resource allocation and packet scheduling algorithm for fourth-generation cellular networks is proposed to maximize the video quality [15]. In [16], a joint video packet scheduling and power allocation algorithm over downlink orthogonal division multiple-access systems is presented to of all MTs under delay-bound constraints. In [17], a cross-layer video packet scheduling algorithm is proposed for minimizing the reconstructed video distortion at each MT to guarantee the fairness among different MTs. In [18], a joint video packet scheduling and playout control framework with the Markov decision process is formulated, and a novel content-aware playout control algorithm is proposed. In [19], a distortion-aware video packet scheduling algorithm over wireless networks is proposed. For cognitive radio networks, a maximum average service rate and optimal packet queue scheduling algorithm is proposed with delay-constrained video communication in Nakagami fading channels [20].

At heterogeneous wireless networks, an energy and content-aware video packet scheduling algorithm with multihoming technology is proposed to consider the energy limitation and the required video quality of service (QoS) [24]. In [23], a joint rate control and scalable stream adaptation problem for

Manuscript received July 21, 2016; revised November 11, 2016 and January 7, 2017; accepted January 22, 2017. Date of publication January 25, 2017; date of current version August 11, 2017. This work was supported in part by the National Natural Science Foundation of China under Grant 61301108, Grant 61671244, and Grant 61640020; in part by the Project of Jiangsu Provincial Six Talent Peaks (no. XYDXXJS-033); and in part by the Jiangsu Province Key Research and Development Plan (BE2016368-1). The review of this paper was coordinated by Dr. N.-D. Dao.

L. Xu and Y. Yang are with the School of Computer Science and Engineering, Nanjing University of Science and Technology, Nanjing 210094, China (e-mail: xulei_marcus@126.com; yuwangyang@126.com).

A. Nallanathan is with the Department of Informatics, King's College London, London WC2R 2LS, U.K. (e-mail: nallanathan@ieee.org).

Color versions of one or more of the figures in this paper are available online at http://ieeexplore.ieee.org.

Digital Object Identifier 10.1109/TVT.2017.2657800

[1] In this paper, CSI is equal to the channel power gain.

TABLE I
SUMMARY OF IMPORTANT SYMBOLS

Symbol	Definition
$\mathcal{F}$	Set of frames
$\mathcal{T}$	Set of timeslots
$\mathcal{N}$	Set of wireless networks
$\mathcal{L}_f$	Set of packets at frame f
$\mathcal{A}_l^f$	Set of ancestors for each packet l_f
$\mathcal{S}_n^*$	Set of primary BSs in primary network n
$\mathcal{S}_n$	Set of secondary BSs in cognitive network n
$\mathcal{M}$	Set of secondary MTs in this geographical region
$\mathcal{M}_{\rm ns}$	Set of secondary MTs in cognitive network n BS s
n_0	Noise power spectral density
E_m	Total available energy at MT m
$\eta_{\rm nsm}$	Power amplifier coefficient
N	Number of cognitive wireless networks
$x_{\rm nsm}^{\rm fl}$	Video packet scheduling decision
S_n^*	Number of primary BSs in primary network n
S_n	Number of secondary BSs in cognitive network n
M	Number of secondary MTs in this geographical region
$M_{\rm ns}$	Number of secondary MTs in cognitive network n BS s
$\tilde{T}_c^m$	Upper bound of video call time for secondary MT m
$I_{\rm ns}$	Interference threshold for cognitive network n BS s
$P_{\rm nsm}$	Power for cognitive network n BS s MT m
$B_{\rm nsm}$	Bandwidth for cognitive network n BS s MT m
$R_{\rm nsm}$	Rate for cognitive network n BS s MT m
$CW_{\rm nsm}$	Capacity for cognitive network n BS s MT m
P_c	Fixed circuit power for each secondary MT's interface

multiple clients concurrently is formulated, and randomized packet scheduling algorithm is proposed. Although the video packet scheduling problems for heterogeneous wireless networks are investigated in [23] and [24], how video traffic with stochastic QoS requirement affects the power allocation and video packet scheduling for cognitive heterogeneous networks needs to be further investigated.

In this paper, we investigate the video transmission framework with stochastic QoS requirement for cognitive heterogeneous wireless networks. Specially, we summarize our contributions as follows.

1) The video packet scheduling problem based on auction theory is formulated to maximize the video quality.
2) A heuristic packet scheduling scheme is proposed and a video quality cumulative distribution function (CDF) is analyzed
3) A power allocation problem is formulated to maximize the minimization lower bounder of video quality during the target call duration, and particle swarm optimization (PSO)-based algorithm is proposed to allocate the power among different secondary MTs.

Simulation results demonstrate that video scheduling and power allocation algorithms improve the video quality and strike the balance between fairness and stochastic video quality.

The rest of this paper is organized as follows. The system model is described in Section II. Section III presents the video packet scheduling and the video quality CDF analysis. A power allocation algorithm with stochastic QoS guarantee is given in Section IV. Finally, performance evaluation and conclusions are given in Sections V and VI, respectively. Table I summarizes the important mathematical symbols used in this paper.

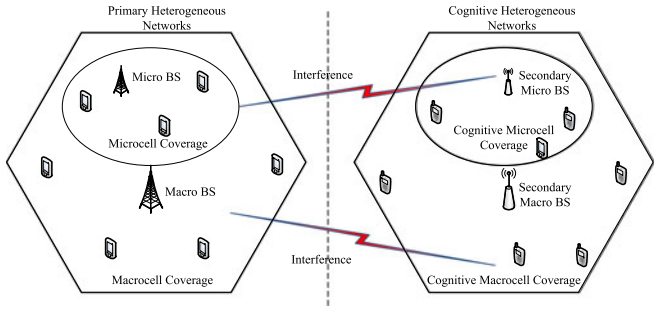

Fig. 1. Cognitive heterogeneous networks.

II. SYSTEM MODEL

In this section, system model is described first. Then, power consumption model and transmission rate model are presented. Finally, packet-level model and call-level model for video traffic are given.

A. System Description

In this paper, there is a set, $\mathcal{N} = \{1, 2, \ldots, N\}$, of wireless networks operated by different service providers. In each wireless network, there is a set, $\mathcal{S}_n = \{1, 2, \ldots, S_n\}$, of secondary base stations (BSs) and a set, $\mathcal{S}_n^* = \{1, 2, \ldots, S_n\}$, of primary BSs in the geographical region. Since the coverage of secondary BSs for each network is different from each other and different cognitive networks have overlapped coverage in some areas, the geographical region is partitioned into multiple service areas, as shown in Fig. 1. There is a set, $\mathcal{M} = \{1, 2, \ldots, M\}$, of secondary MTs in the geographical region and $\mathcal{M}_{\rm ns} = \{1, 2, \ldots, M_{\rm ns}\} \in \mathcal{M}$ is a subset of secondary MTs in the coverage area of cognitive network n BS s. In the same cognitive network, interference mitigation is achieved by interference management schemes [19], [25]. Using internetwork cooperation and multiple radio interfaces, each secondary MT can communicate with multiple secondary BSs simultaneously.

In this paper, primary MTs and secondary MTs can share the same spectrum, and the interference power should be controlled to protect the primary MTs' communication. The interference power at each primary BS is controlled with the interference temperature model [26]. Additionally, video traffic transmission is considered [27], [28]. At each time slot, secondary MTs allocate power $P_{\rm nsm}^k$ for cognitive network n BS s MT m at subcarrier k and video packet scheduling decision $x_{\rm nsm}^{\rm fl}$. If packet l of frame f is assigned to cognitive network n BS s MT m, $x_{\rm nsm}^{\rm fl} = 1$; otherwise, $x_{\rm nsm}^{\rm fl} = 0$. The video transmission decision policy on $P_{\rm nsm}^k$ and $x_{\rm nsm}^{\rm fl}$ is obtained according to the video traffic characteristics, CSI among different interfaces, and secondary MT total energy constraint. The CSI is unchanged at one time slot and is different from one time slot to another.

B. Power Consumption and Transmission Rate Model

The power consumption at each interface for each secondary MT has two parts. The first part is a fixed circuit power for each secondary MT's interface and is given by P_c. The second part is

a dynamic part with the digital circuit power consumption and the allocated transmission bandwidth

$$P_{\text{nsm}}^{\text{T}} = \frac{P_{\text{nsm}}}{\eta_{\text{nsm}}} + P_c \tag{1}$$

where P_{nsm} is the allocated power for cognitive network n BS s to communicate secondary MT m, and η_{nsm} is the power amplifier coefficient for cognitive network n BS s MT m.

The transmission rate at the physical layer for cognitive network n BS s MT m is

$$R_{\text{nsm}} = B_{\text{nsm}} \log_2 \left(1 + \frac{P_{\text{nsm}} g_{\text{nsm}}}{B_{\text{nsm}} n_0 + I_{\text{nsm}}}\right). \tag{2}$$

where g_{nsm} is the channel power gain between secondary MT m and cognitive network n BS s, B_{nsm} is the bandwidth for cognitive network n BS s MT m, I_{nsm} is the interference power caused by primary MTs for cognitive network n BS s MT m, and n_0 is one-sided spectral density of noise power [29].

C. Packet-Level Model for Video Traffic

A video bit stream is encoded with a layered video encoder, i.e., a base layer and several enhancement layers are encoded, and each layer is encoded via a group of picture (GoP).[2] At the same time slot, the data are encoded interdependently with estimated motion [26]. However, data with different time slots are encoded independently [33]. Time is divided with time slots, $\mathcal{T} = \{1, 2, \ldots, T\}$, and the time slot duration, τ, is equal. We adopt video call duration to estimate T. Each time slot contains $\mathcal{F} = \{1, 2, \ldots, F\}$ frames from different layers, and each frame is of I, P, or B type. Each frame contains packets and each packet has the video bit stream at one frame. For example, frame f contains L_f packets, $\mathcal{L}_f = \{1, 2, \ldots, L_f\}$, and each packet has length h_f bits. In packet-level model for video traffic, some frames are relative to other frames, and these frames exist dependencies. Consequently, decoding video packets at one frame relies on the successful video packet decoding from other frames. The video packets dependencies at different frames are depicted with a directed acyclic graph [24]. Consequently, each packet l_f has a video packet set of ancestors $\mathcal{A}_l^f$. Video packets at $\mathcal{A}_l^f$ have smaller delay deadline and higher impact than video packet l_f [26].

D. Call-Level Model for Video Traffic

Assume call arrivals for video traffic follow a Poisson process, and the arrival rate for both new and handoff video calls is λ. Since the most calls for video traffic have a short duration, and a small fraction of calls are a large duration, the video call duration is modeled as a heavy-tailed distribution with hyperexponential distributions [26]. In this paper, a hyperexponential distribution with two-stage mode is adopted for the call duration, and probability density function (PDF) for the video call duration T_c^m at secondary MT m is

$$f_{T_c^m}(t) = \frac{a^2}{(a+1)\,\overline{T}_c^m} e^{-\frac{a}{\overline{T}_c^m} t} + \frac{1}{a\,(a+1)\,\overline{T}_c^m} e^{-\frac{1}{a\,\overline{T}_c^m} t} \tag{3}$$

where $\overline{T}_c^m$ is the mean, and a characterizes the mice-elephant feature [34].

In the service area, the user residence time for the mobility of the secondary MT m at the service area T_r^m is assumed to be exponential distribution. Additionally, the channel holding time is $T_h^m = \min(T_c^m, T_r^m)$, and its PDF is

$$\begin{aligned} f_{T_h^m}(t) = {} & \frac{a}{(a+1)} \left(\frac{1}{\bar{T}_r^m} + \frac{a}{\bar{T}_c^m}\right) e^{-\left(\frac{1}{\bar{T}_r^m} + \frac{a}{\bar{T}_c^m}\right) t} \\ & + \frac{1}{(a+1)} \left(\frac{1}{\bar{T}_r^m} + \frac{1}{a\bar{T}_c^m}\right) e^{-\left(\frac{1}{\bar{T}_r^m} + \frac{1}{a\,\bar{T}_c^m}\right) t} \end{aligned} \tag{4}$$

where T_c^m and T_r^m are independent of each other, and $\overline{T}_r^m$ is the mean for the user resident time, and the derivation of (4) can be obtained in [34].

III. Video Packet Scheduling and Analysis

In this section, a video packet scheduling problem is formulated first. Then, a video packet scheduling scheme based on auction is proposed. Finally, the CDF for video quality at each secondary MT is analyzed.

A. Video Packet Scheduling Problem Formulation

In cognitive heterogeneous wireless networks, each secondary MT can utilize radio resource allocation from different cognitive networks to achieve the better performance with the internetwork cooperation technology. The decoder time stamp difference between two consecutive frames for the delay deadline is constant, $|d_{f+1} - d_f| = \Delta D$. Additionally, the delay deadline of video packets at the same frame are same. Consequently, the minimum transmission rate requirement for packet, $l_f\ \forall f \in \mathcal{F}$, is $r(l_f) = h_f / \Delta D$. The overall transmission rate requirement for video packet at a radio interface satisfies the achieved transmission rate, i.e.,[3]

$$\sum_{l_f \in \mathcal{L}_f} \sum_{f \in \mathcal{F}} x_{\text{nsm}}^{\text{fl}} r(l_f) \le R_{\text{nsm}} \tag{5}$$

where R_{nsm} is the achieved transmission rate for cognitive network n BS s MT m.

With the dependence among different video packets, packets, whose ancestors are not transmitted, are not transmitted, i.e.,

$$x_{\text{nsm}}^{\text{fl}} \le x_{n^* s^* m}^{f^* l^*}, \forall l_{f^*}^* \in A_l^f, l_f \in \bigcup_{f \in \mathcal{F}} \mathcal{L}_f. \tag{6}$$

[2]Video coding is an important measurement to improve received video quality with dynamic channel conditions for cognitive heterogeneous networks. Since we focus on the power allocation and video packet scheduling problem with stochastic QoS guarantee, we adopt the layered video encoder, which can be applied to a general one, e.g., H.264/MPEG-4 [30]–[32], instead of investigating the video coding optimization. The conclusion of our paper can be applied to the video coding optimization problem easily.

[3]If the practical transmission rate of the scheduled video packets at a radio interface is no larger than the maximum transmission rate, we assume the scheduled video packets can be transmitted correctly between the secondary MT and secondary BS; otherwise, we drop the extra video packets with less video quality impact. This assumption makes the joint video packet scheduling and power allocation problem is analyzed conveniently.

Additionally, a video packet is assigned to at most one radio interface, i.e.,

$$\sum_{n\in\mathcal{N}}\sum_{s\in\mathcal{S}_n} x_{\text{nsm}}^{\text{fl}} \le 1. \tag{7}$$

The optimization framework maximizes the perceived video service quality, which is achieved via video packet scheduling, i.e.,

$$OP1: \max_{x_{\text{nsm}}^{\text{fl}}} \left\{ q_m = \frac{\sum_{n\in\mathcal{N}}\sum_{s\in\mathcal{S}_n}\sum_{l_f\in\mathcal{L}_f}\sum_{f\in\mathcal{F}} v_f^l x_{\text{nsm}}^{\text{fl}}}{\sum_{n\in\mathcal{N}}\sum_{s\in\mathcal{S}_n}\sum_{l_f\in\mathcal{L}_f}\sum_{f\in\mathcal{F}} v_f^l} \right\} \tag{8}$$

$$\text{s.t.} \quad (5),(6),(7), x_{\text{nsm}}^{\text{fl}} \in \{0,1\}.$$

where v_f^l is the impact weight of video packet quality for the packet l at the frame f. Problem (8) considers the video characteristics based on delay deadlines, distortion impact, video packet dependence, and the CSI for the multiple radio interfaces.

In this formulation, the transmission rate characters the capacity for each secondary MT's interference. The packet delay guarantees the quality for each video packet. If the waiting time for a video packet exceeds its maximum delay, it will be dropped. In order to maximize the video transmission quality, we need to reduce the packet loss probability. Therefore, it is necessary to design an efficient video packet scheduling algorithm to reduce the packet loss probability.

B. Video Packet Scheduling Scheme Based on Auction

In this paper, auction theory is a natural way in constructing economic model for video packet scheduling. In the auction model, video packet auctioneer exists to run the auction, determine the winners, optimally assign the resources, and charge the payments. At each secondary MT, each radio interface has a set of subchannels to serve its allocated video packets. At the beginning of this auction, each radio interface at secondary MT submits the total achieved transmission rate to the video packet auctioneer, and each secondary MT sends out its private information including its video packets and its bidding price for each video packet. The video packet auctioneer collects all these sealed-bid information and determines an optimal video packet scheduling scheme. Additionally, the video packet auctioneer calculates the payments and payoffs for video packets and each radio interface.

In this auction model, $\mathcal{NS}$, with $|\mathcal{NS}| = NS$ is a set of radio interfaces, $\mathcal{CW}_m = \{CW_{\text{nsm}}\}, n \in \mathcal{N}, s \in \mathcal{S}_n$ is a set of the auctioned capacity, and $CW_{\text{nsm}} = R_{\text{nsm}}\tau$ is the capacity for cognitive network n BS s MT m. Additionally $\mathcal{LF}$ with $|\mathcal{LF}| = LF$ is a set of video packets, $r(l_f) = h_f/\Delta D_{f+1,f}$ is a specific transmission rate requirement for each video packet, and $\Delta D_{f+1,f} = |d_f - d_{f+1}|$ is the delay difference between any two consecutive frames. Video packets at the same frame f have the same delay deadline, denoted by d_f, and the private valuation for each video packet is v_f.

Obviously, there is one seller with video packets, radio interfaces are bidders, and the set of bid bundles is $\mathcal{BW}_m = \{BW_{\text{nsm}}\}, n \in \mathcal{N}, s \in \mathcal{S}_n$. Each bid B_{nsm} is specified as a 2-tuple $(d_{\text{nsm}}, pv_{\text{nsm}})$, where d_{nsm} is the transmission rate requirement for each bidder, and pv_{nsm} is the amount that the bidder is willing to pay for d_{nsm}. For truthful auction, the bidding price is equal to true valuation. The content-aware packet scheduling (CAPS) is presented in Algorithm 1. In CAPS, rc_{nsm} is the remaining capacity for cognitive network n BS s MT m, $\mathcal{A}_i$ is the ith group of video packets, $\mathcal{AV}$ is the distortion impact of video packets, and $\mathcal{A}$ is the set of the allocated video packets.

Algorithm 1: Content-Aware Packet Scheduling (CAPS).

Require: Input CW_{nsm} and $l_f, \quad \forall f \in \mathcal{F}$.
Ensure: Output x_{nsm}^{fl}.

1: Secondary MTs advertise video packets $l_f, \quad \forall l_f \in \mathcal{L}_f$, $f \in \mathcal{F}$ for auction, and $\text{rc}_{nsm} = R_{nsm}\tau$.
2: Divide all video packets into different groups, and the video packets with dependence are divided into a group. There are AN groups.
3: **repeat**
4: Put the first packet of each group into the set $\mathcal{A} = \{\mathcal{A}_i(1)\}$, compute $\mathcal{AV} = \{\mathcal{A}_i(1)v_f^{\mathcal{A}_i(1)}\}$, $i = 1, 2, \ldots, AN$.
5: Secondary MT receives bids $\mathcal{BW}_m = \{BW_{nsm}\}$ from radio interfaces.
6: Select the video packet, $(f^*, l^*) = \max_{l_f\in\mathcal{L}_f, f\in\mathcal{F}} \mathcal{AV}$, with the largest distortion impact. Select the radio interface, $(n^*, s^*) = \max_{n\in\mathcal{N}, s\in\mathcal{S}_n} \text{rc}_{nsm}$, with the largest remaining capacity.
7: **if** $\text{rc}_{n^*s^*m} - r(l_{f^*}^*) \ge 0$ **then**
8: Set $x_{n^*s^*m}^{f^*l^*} = 1$, delete the video packet, (f^*, l^*), from the set $\mathcal{A}$, $\mathcal{AV}$, and $\mathcal{A}_i$. Update the remaining capacity, $\text{rc}_{n^*s^*m} = R_{n^*s^*m}\tau - r(l_{f^*}^*)$. Go to step 4.
9: **else**
10: Output x_{nsm}^{fl}.
11: **end if**
12: **until**

C. Video Quality CDF

In the section, the video quality q_m given the secondary MT transmission rates R_{nsm} at different radio interfaces and frame size c_f is obtained first. Then, using the data rates and packet encoding statistics, the CDF of video quality, $F_{Q_m}(q_m)$, is analyzed. With CAPS, the video quality q_m is obtained using transmission rates R_{nsm} and frame size c_f.

The set of different video packet encoding and transmission rate combinations resulting in the same video service quality q_m is $\mathcal{Q}_m$, and the transmission rate and frame size statistics are mapped into a probability mass function (PMF) for video quality, i.e.,

$$F_{Q_m}(q_m) = \sum_{\mathcal{Q}_m} f_{\mathcal{X}_R}(\mathcal{X}_r) f_{C_I,C_B,C_P}(c_I, c_B, c_P) \tag{9}$$

where $f_{C_I,C_B,C_P}(c_I, c_B, c_P)$ is the joint PMF for packet encoding at I, B, and P frames with independent and identically distributed frame size statistics [24] $\mathcal{X}_R = [R_{11m}, \ldots, R_{NS_N m}]$,

$\mathcal{X}_r = [r_{11m}, \ldots, r_{NS_N m}]$, $\mathcal{X}_B = [B_{11m}, \ldots, B_{NS_N m}]$, and $\mathcal{X}_b = [b_{11m}, \ldots, b_{NS_N m}]$.

For independent fading statistics at different interfaces, the probability about transmission rates, $r_{11m}^{i_{11m}}, \ldots, r_{NS_N m}^{i_{NS_N m}}$, is

$$f_{\mathcal{X}_R|\mathcal{X}_B}(\mathcal{X}_r) = \sum_{\mathcal{B}_m} f_{\mathcal{X}_B}(\mathcal{X}_b) f_{\mathcal{X}_R|\mathcal{X}_B}(\mathcal{X}_r|\mathcal{X}_b) \tag{10}$$

where $\mathcal{B}_m$ is the allocated bandwidth set to secondary MT m. The conditional probability for transmission rates, $r_{11m}^{i_{11m}}, \ldots, r_{NS_N m}^{i_{NS_N m}}$, at radio interfaces, given the bandwidth allocation $B_{11m}, B_{12m}, \ldots, B_{NS_N m}$, is

$$f_{\mathcal{X}_R|\mathcal{X}_B}(\mathcal{X}_r|\mathcal{X}_b) = \prod_{n\in\mathcal{N}, s\in\mathcal{S}_n} f_{R_{\text{nsm}}^{i_{\text{nsm}}}|B_{\text{nsm}}}\left(r_{\text{nsm}}^{i_{\text{nsm}}}|b_{\text{nsm}}\right). \tag{11}$$

Given the allocated bandwidth B_{nsm}, the conditional probability about the transmission rate $r_{\text{nsm}}^{i_{\text{nsm}}}$ for cognitive network n BS s MT m is

$$f_{R_{\text{nsm}}^{i_{\text{nsm}}}|B_{\text{nsm}}}\left(r_{\text{nsm}}^{i_{\text{nsm}}}|b_{\text{nsm}}\right) = \Pr\left(\Gamma_{\text{nsm}}^{i_{\text{nsm}}+1} > \gamma_{\text{nsm}} \geq \Gamma_{\text{nsm}}^{i_{\text{nsm}}}\right) \tag{12}$$

where the received signal-to-interference-plus-noise rate (SINR) γ_{nsm} for cognitive network n BS s MT m is an exponential distribution, $\overline{\gamma}_{\text{nsm}} = P_{\text{nsm}}\Omega_{\text{nsm}}/B_{\text{nsm}}n_0$ is the average received SINR for secondary MT m to communicate with cognitive network n BS s, Ω_{nsm} is the average channel power gain for secondary MT m to communicate with cognitive network n BS s, and $\Gamma_{\text{nsm}}^{i_{\text{nsm}}}$ is the i_{nsm}th SINR threshold.

Each radio interface for secondary MT m can support a discrete transmission rate set $r_{\text{nsm}}^{i_{\text{nsm}}}$ with $i_{\text{nsm}} \in \{1, \ldots, I\}$. This interface can support transmission rate if the received SINR γ_{nsm} at this radio interface exceeds a given threshold $\Gamma_{\text{nsm}}^{i_{\text{nsm}}}$. The threshold set $\Gamma_{\text{nsm}}^{i_{\text{nsm}}}$, $n \in \mathcal{N}, s \in \mathcal{S}_n, m \in \mathcal{M}, i_{\text{nsm}} \in \mathcal{I}$ is calculated by

$$\Gamma_{\text{nsm}}^{i_{\text{nsm}}} = 2^{\frac{r_{\text{nsm}}^{i_{\text{nsm}}}}{B_{\text{nsm}}}} - 1, i_{\text{nsm}} \in \mathcal{I} \tag{13}$$

where $\Gamma_{\text{nsm}}^{I+1}$ is assumed to be ∞.

IV. Power Allocation With Stochastic QoS

In this section, a power allocation problem with maximizing the minimization video quality lower bound is formulated first. Then, a power allocation algorithm based on PSO is proposed for cognitive heterogeneous networks.

A. Power Allocation Problem Formulation

From (10), the probability for the transmission rates R_{nsm} at different interfaces depends on the received average SINR $\overline{\gamma}_{\text{nsm}}$. Consequently, the CDF of video quality is a function of the allocated bandwidth and power at different interfaces. The total power consumption for secondary MT m satisfies the maximum power constraint condition, i.e.,

$$\sum_{n\in\mathcal{N}} \sum_{s\in\mathcal{S}_n} \left(P_c + \frac{P_{\text{nsm}}}{\eta_{\text{nsm}}}\right) \leq \frac{E_m}{\widetilde{T}_c^m} \tag{14}$$

where E_m is the total available energy at MT m, and $\widetilde{T}_c^m$ is the upper bound of video call time for secondary MT m, i.e.,

$$\Pr\left(T_c^m \leq \widetilde{T}_c^m\right) \geq 1 - \varepsilon_c^m, \varepsilon_c^m \in [0, 1]. \tag{15}$$

where ε_c^m is the lower bound of video call time for secondary MT m.

The interference power at primary BS is limited by

$$\mathrm{E}\left(\sum_{m\in\mathcal{M}_{\text{ns}}} P_{\text{nsm}} h_{\text{nsm}}^{\text{PBS}}\right) \leq I_{\text{ns}} \tag{16}$$

where I_{ns} is the interference threshold for primary network n BS s, and $h_{\text{nsm}}^{\text{PBS}}$ is the channel power gain between secondary MT m and primary network n BS s with an exponential distribution.

The power allocation strategy adapts to the channel condition to maximize the minimum lower bound of video quality among different secondary MTs under the QoS requirement, i.e.,

$$\begin{aligned} \text{OP2}: &\max_{P_{\text{nsm}}} \{\min q_m\} \\ \text{s.t.}: &\, C1. F_{Q_m}(q_m) \leq \varepsilon_q \\ &\, C2.\ (14), (15), P_{\text{nsm}} \geq 0 \end{aligned} \tag{17}$$

where ε_q is a parameter for the balance between the desired performance and the successful probability of the call transmission.

In this paper, we do not consider the combination of $x_{\text{nsm}}^{\text{fl}}$ and P_{nsm} as a target solution. There are three reasons. First, joint video packet scheduling and power allocation problem is an NP-hard problem. It is difficult to solve the optimal solution. Usually, the original NP-hard problem is divided into subproblems. Then, the objective functions in (8) and (17) are different. The objective function in (8) maximizes the video quality for secondary MT m via the video packet scheduling, whereas the objective function in (17) maximizes the minimization video packet quality among M secondary MTs. Finally, the video packet scheduling algorithm affects the analysis of video quality CDF. Additionally, the video packet CDF affects the design of the power allocation algorithm.

B. Power Allocation Scheme

The power allocation problem (17) is nonconvex optimization problem, and swarm intelligence algorithm can be used to solve it. In swarm intelligence algorithms, PSO is an optimization technique based on the sociological behavior associated with birds flocking. This seeking behavior is an optimization search for solutions to nonlinear equations. In PSO, a potential solution in the fitness landscape is called a particle, and a particle representation in swarm is depicted in Fig. 2. In Fig. 2, a particle length is $M|\mathcal{M}_{\text{ns}}|$, and each particle includes the position vector and the velocity vector. For example, the ith particle $\mathcal{X}_i(t) = [x_i^1(t), \ldots, x_i^d(t), \ldots, x_i^{M|\mathcal{M}_{\text{ns}}|}(t)]$ is associated with a velocity vector $\mathbf{v}_i(t) = [v_i^1(t), \ldots, v_i^d(t), \ldots, v_i^{M|\mathcal{M}_{\text{ns}}|}(t)]$. Each particle changes its searching direction based on two values during each iteration. The first one is the best searching experience of individual $\mathcal{X}_{\text{pbest}_i}(t)$. The second one is the best result

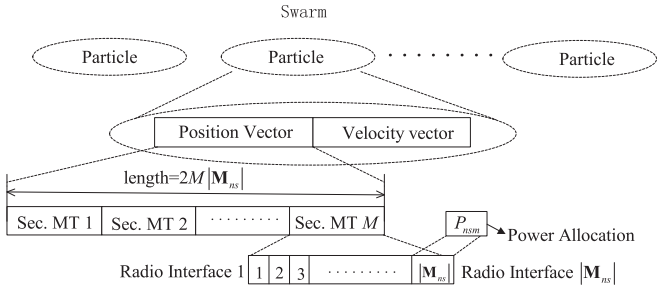

Fig. 2. Particle representation in swarm.

Algorithm 2: Power Allocation Scheme (PAS).

Require: Input ε_q, B_{ns}, E_m and I_{ns}.
Ensure: Output P_{nsm}.
1: Generate the initial swarms which satisfy the constraints in (17).
2: **repeat**
3: Calculate the fitness value $f\left(\mathcal{X}_i\left(t\right)\right)$ of the current position for each particle in swarm.
4: **if** $f\left(\mathcal{X}_i\left(t\right)\right) > f\left(\mathcal{X}_{pbest_i}\left(t\right)\right)$ **then**
5: Set $\mathcal{X}_{pbest_i}\left(t\right) = \mathcal{X}_i\left(t\right)$.
6: **end if**
7: **if** $f\left(\mathcal{X}_i\left(t\right)\right) > f\left(\mathcal{X}_{gbest}\left(t\right)\right)$ **then**
8: Set $\mathcal{X}_{gbest}\left(t\right) = \mathcal{X}_i\left(t\right)$.
9: **end if**
10: Update the position and velocity for each particle. Moreover, update the inertia weight $\psi\left(t\right)$. Set $t \leftarrow t+1$, and go to step 2.
11: **until** $t \leq T_{\max}$
12: Report $\mathcal{X}_{gbest}\left(t\right)$ as the optimal solution.

obtained by any particle in the swarm $\mathcal{X}_{\text{gbest}}\left(t\right)$. When $\mathcal{X}_{\text{pbest}_i}\left(t\right)$ and $\mathcal{X}_{\text{gbest}}\left(t\right)$ are obtained, the ith particle updates its velocity and position by

$$v_i^d\left(t+1\right) = \psi\left(t\right) v_i^d\left(t\right) + \eta_1 r_1 \left[x^d_{\text{pbest}_i}\left(t\right) - x_i^d\left(t\right)\right] + \eta_2 r_2 \left[x^d_{\text{gbest}}\left(t\right) - x_i^d\left(t\right)\right] \tag{18}$$

and

$$x_i^d\left(t+1\right) = x_i^d\left(t\right) + v_i^d\left(t\right) \tag{19}$$

where $v_i^d\left(t+1\right)$ and $v_i^d\left(t\right)$ are the dth dimension velocities of particle i at the $(t+1)$th and tth iterations, respectively. $x_i^d\left(t+1\right)$ and $x_i^d\left(t\right)$ are the dth dimension positions of particle i at the tth and $(t+1)$th iterations, respectively. $\mathcal{X}_{\text{pbest}_i}\left(t\right)$ and $\mathcal{X}_{\text{gbest}}\left(t\right)$ are the best position found by particle i and the best position found by the whole swarm at the tth iteration, respectively. η_1 and η_2 are the acceleration constants. r_1 and r_2 are the random numbers generated in the interval $[0, 1]$. In (18), $\psi\left(t\right)$ is the inertia weight updated by

$$\psi\left(t+1\right) = \psi\left(1\right) + \left[\psi\left(T_{\max}\right) - \psi\left(1\right)\right] \frac{e^{m_i(t)} - 1}{e^{m_i(t)} + 1} \tag{20}$$

and

$$m_i\left(t\right) = \frac{f\left(\mathcal{X}_{\text{pbest}_i}\left(t\right)\right) - f\left(\mathcal{X}_i\left(t\right)\right)}{f\left(\mathcal{X}_{\text{pbest}_i}\left(t\right)\right) + f\left(\mathcal{X}_i\left(t\right)\right)} \tag{21}$$

where $\psi\left(t+1\right)$ and $\psi\left(t\right)$ are the inertia weights at the $(t+1)$th and tth iterations, respectively. $T_{\max}$ is the maximum iteration number and $m_i\left(t\right)$ is the relative improvement function at the tth iteration. The fitness function for $\mathcal{X}_i\left(t\right)$ is

$$f\left(\mathcal{X}_i\left(t\right)\right) = \min_{m \in \mathcal{M}} q_m. \tag{22}$$

C. Computational Complexity

In CAPS, the computational complexity is $O(\sum_{n\in\mathcal{N}} \sum_{s\in\mathcal{S}_n} 3N^P_{\text{nsm}})$. N^P_{nsm} is the number of allocated video packets for cognitive network n BS s MT m. In PAS, assume N_g is the total iteration number in PSO, N_j^i is the cyclic number of the jth particle at the ith iteration for generating the feasibility of power allocation, and N_p is the population number in PSO. Consequently, the total time complexity is $O(\sum_{i=1}^{N_g} \sum_{j=1}^{N_p} 8N_j^i)$.

V. Performance Evaluation

This section presents the simulation results for proposed algorithms for video transmission problem with stochastic QoS requirement. We consider a geographical region covered by one cognitive macrocell and one cognitive microcell. The cognitive macrocell has a radius 400 m at the coverage area, whereas the cognitive microcell has a radius 200 m at the coverage area. Due to the overlapped coverage between cognitive macrocell and cognitive microcell, two service areas can be distinguished and secondary MTs can get service from both cognitive macrocell BS and cognitive microcell BS. The path loss exponent is 4, and the amplitude of multipath fading is Rayleigh. The noise power is 7×10^{-10} W, and I_{nsm} follows $N\left(0, 1 \times 10^{-11}\right)$ W. The other simulation parameters are $\eta_{\text{nsm}} = 0.35$, and $Q_{\text{nsm}} = 10$ mW. The number of secondary MTs in cognitive macrocell and cognitive microcell are 2, respectively. To compare with CAPS+PAS, an earliest deadline first approach (EDFA) is adopted [25]. Video sequences are compressed with an MPEG4-FGS encoder, at 30 ft/s with the GoP structure. The GoP structure includes 14 frames from one layer. Additionally, τ is 466 ms, and the decoder time stamp difference between two successive frames for the delay deadline is $\Delta D = 40$ ms. The bandwidths of cognitive macrocell and cognitive microcell are both $B_{\text{ns}} = 4$ MHz. Each packet at video traffic requires a transmission data rate 2 kb/s. The values for video packet distortion impact are $v_f^l = 4$ for P frames, $v_f^l = 2$ for B frames, and $v_f^l = 5$ for I frames [26]. For simplicity, the parameters for sample PMFs of I, B, and P frame sizes are adopted in [26].

The allocated bandwidth for different secondary MTs on the two radio interfaces can be described as

$$\mathcal{B}_{111} = \begin{bmatrix} 1 & 0.5 & 0.375 & 0.25 & 0.125 \\ 1.5 & 1 & 0.75 & 0.5 & 0.25 \end{bmatrix} \tag{23}$$

$$\mathcal{B}_{112} = \begin{bmatrix} 1 & 1.5 & 1.625 & 1.75 & 1.875 \\ 0.5 & 1 & 1.25 & 1.5 & 0.175 \end{bmatrix} \tag{24}$$

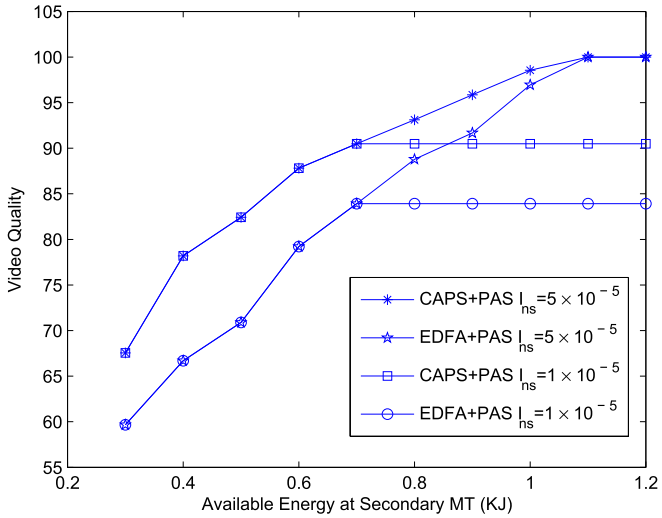

Fig. 3. Video quality versus secondary MT available energy.

$$\mathcal{B}_{211} = \begin{bmatrix} 1.25 & 1.5 & 1.375 & 0.75 & 0.5 \\ 1 & 1.25 & 0.75 & 1.25 & 1.5 \end{bmatrix} \quad (25)$$

and

$$\mathcal{B}_{212} = \begin{bmatrix} 0.75 & 0.5 & 0.625 & 1.25 & 1.5 \\ 1 & 0.75 & 1.25 & 0.75 & 0.5 \end{bmatrix} \quad (26)$$

where the first and second rows in $\mathcal{B}_{111}$, $\mathcal{B}_{112}$, $\mathcal{B}_{211}$, and $\mathcal{B}_{212}$ are the offered bandwidths on the first and second interfaces of different secondary MTs, respectively. $f_{B_{111},\ldots,B_{212}} = \begin{bmatrix} 0.4371 & 0.2109 & 0.1217 & 0.1023 & 0.1280 \end{bmatrix}$ is the probability that the bandwidths are offered to secondary MTs and each entry in $f_{B_{111},\ldots,B_{212}}$ corresponds to a column in $\mathcal{B}_{111}$, $\mathcal{B}_{112}$, $\mathcal{B}_{211}$, and $\mathcal{B}_{212}$. The set of transmission rates supported at each interface is $\mathcal{R} = \{0.1k, k = 0, 1, \ldots, 25\}$ Mb/s. With (14), $\mathcal{R}$ is supported at the two different radio interfaces with different thresholds, for different allocated bandwidths and for different secondary MTs. Each interface has average channel power gain defined by

$$\mathbf{\Omega} = \begin{bmatrix} 0.7123 & 0.5031 & 0.4126 & 0.6913 \\ 0.6713 & 0.4852 & 0.4714 & 0.7210 \end{bmatrix}. \quad (27)$$

We evaluate the impact of video quality on available energy at secondary MT in Fig. 3. The average call duration is $T_c = 20$ min, and the call arrival rate to service area is $\lambda = 0.5$ call/min. Set $\varepsilon_q = 0.9$ and $\varepsilon_c = 0.1$. The interference threshold has two cases, i.e., $I_{\rm ns} = 1 \times 10^{-5}$ W and $I_{\rm ns} = 5 \times 10^{-5}$ W. From Fig. 3, we observe that CAPS+PAS has the larger video quality than EDFA+PAS. Moreover, the video quality for CAPS+PAS and EDFA+PAS increase with the secondary MT's available energy. This is because CAPS exploits the stochastic video quality characteristic, and allows some video packet with low value to be dropped. Consequently, the video quality for CAPS+PAS improves. For the case $I_{\rm ns} = 1 \times 10^{-5}$ W, when secondary MT available energy exceeds a special value, video quality remains unchanged. The reason is that the interference power threshold limits the utilization of secondary MT's available energy.

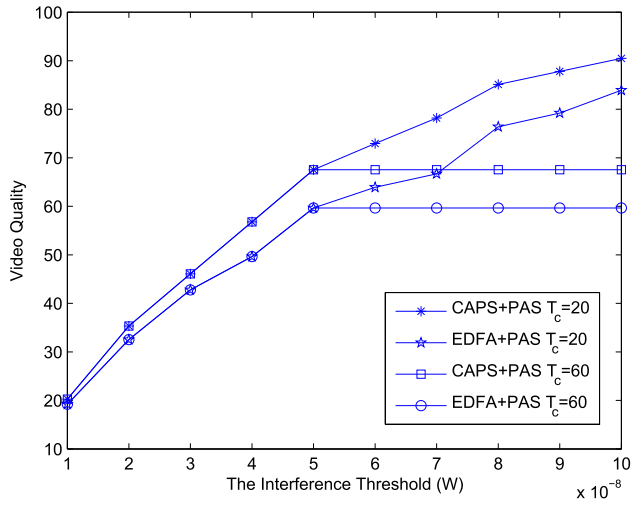

Fig. 4. Video quality versus the interference threshold.

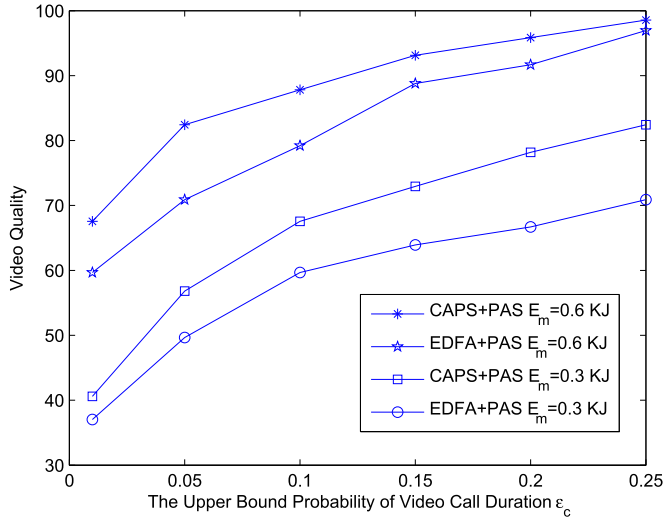

Fig. 5. Video quality versus the upper bound probability of video call duration.

We evaluate the impact of video quality on the interference threshold in Fig. 4. The simulation conditions are $\varepsilon_q = 0.9$ and $\varepsilon_c = 0.1$. The available energy for each secondary MT is $E = 1$ kJ. The average call duration has two cases, i.e., $T_c = 20$ min and $T_c = 60$ min. It can be observed that video quality for CAPS+PAS and EDFA+PAS grow with the interference power threshold. This is because increasing the interference power threshold allows secondary MTs to consume more energy to improve the video quality. It can be also see that video quality of EDFA+PAS is smaller than that of CAPS+PAS. The reason is that, in the EDFA+PAS, video packets whose deadline is closer are scheduled earlier, and it is content independent. For the case $T_c = 60$ min, when the interference threshold exceeds a special value, video quality is unchanged. This can be explained that there is not enough energy to improve the video quality.

We evaluate the impact of video quality on the upper bound probability of video call duration in Fig. 5. The simulation conditions are $\varepsilon_q = 0.9$ and $I_{\rm ns} = 5 \times 10^{-7}$ W. The available energy of each secondary MT has two cases, i.e., $E = 0.3$ kJ and $E = 0.6$ kJ. In Fig. 5, it can be observed that the video

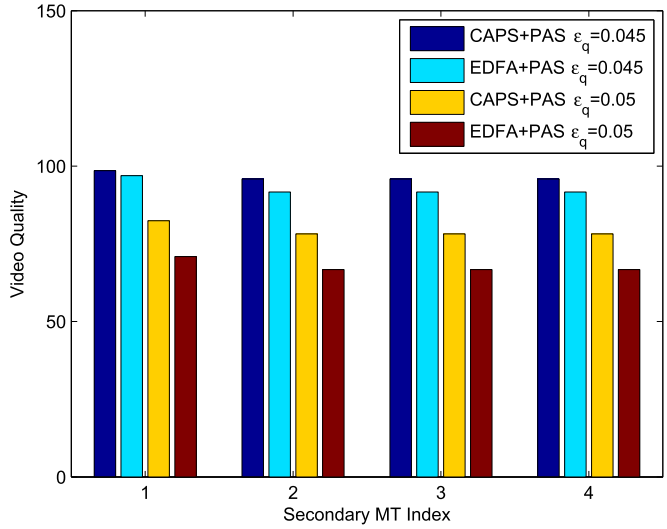

Fig. 6. Video quality versus secondary MT index.

quality for two algorithms grows with the upper bound probability of video call duration. Since increasing the upper bound probability of video call duration not only results in the fact that the operation duration per each charging becomes short, but also leads to increase the available energy consumption of each secondary MT.

We evaluate the fairness of video quality for different algorithms in Fig. 6. The average call duration is $T_c = 40$ min. Set $\varepsilon_c = 0.2$ and $I_{\rm ns} = 5 \times 10^{-7}$ W. There are two cases for the parameter ε_q, i.e., $\varepsilon_q = 0.045$ and $\varepsilon_q = 0.05$. From Fig. 6, we can see that CAPS+PAS and EDFA+PAS can achieve the better fairness to guarantee the video quality among different secondary MTs. This is because PAS allocates power to guarantee the fairness of video quality among different secondary MTs. Although EDFA+PAS can also achieve the fairness very well, its video quality is smaller than that of CAPS+PAS. From Figs. 3–6, it can be concluded that CAPS+PAS not only improves the video quality but guarantees the fairness of video quality among different secondary MTs as well.

VI. Conclusion

In this paper, we investigate the video packet scheduling problem for the sustainable internetwork video transmission over the call duration for cognitive heterogeneous networks. The above optimization problem aims to maximize the lower bound of video quality under the QoS constraints. In order to solve the above stochastic optimization problem, we model the video packet scheduling problem as auction market, and video quality CDF is analyzed. Then, PSO is adopted to adjust the power according to the video stochastic QoS requirement and CSI. The proposed video scheduling framework guarantees the secondary MT to support a required video quality with a certain outage probability over the call duration. Numerical results demonstrate the proposed algorithms can improve the video quality for each secondary MT greatly.

References

[1] H. Xie, F. Gao, S. Zhang, and S. Jin, "A unified transmission strategy for TDD/FDD massive MIMO systems with spatial basis expansion model," *IEEE Trans. Veh. Technol.*, to be published, doi: 10.1109/TVT.2016.2594706.

[2] H. Xie, B. Wang, F. Gao, and S. Jin, "A full-space spectrum-sharing strategy for massive MIMO cognitive radio systems," *IEEE J. Sel. Areas Commun.*, vol. 34, no. 10, pp. 2537–2549, Oct. 2016.

[3] W. L. Huang, K. Letaief, and Y. J. Zhang, "Cross-layer multi-packet reception based medium access control and resource allocation for space-time coded MIMO/OFDM," *IEEE Trans. Wireless Commun.*, vol. 7, no. 9, pp. 3372–3384, Sep. 2008.

[4] A. Furtado, L. Irio, R. Oliveira, L. Bernardo, and R. Dinis, "Spectrum sensing performance in cognitive radio networks with multiple primary users," *IEEE Trans. Veh. Technol.*, vol. 65, no. 3, pp. 1564–1574, Mar. 2016.

[5] C. H. Huang and K. C. Chen, "Dual-observation time-division spectrum sensing for cognitive radios," *IEEE Trans. Veh. Technol.*, vol. 60, no. 8, pp. 3712–3725, Oct. 2011.

[6] K. L. Du and W. H. Mow, "Affordable cyclostationarity-based spectrum sensing for cognitive radio with smart antennas," *IEEE Trans. Veh. Technol.*, vol. 59, no. 4, pp. 1877–1886, May 2010.

[7] S. Stotas and A. Nallanathan, "Optimal sensing time and power allocation in multiband cognitive radio networks," *IEEE Trans. Commun.*, vol. 59, no. 1, pp. 226–235, Jan. 2011.

[8] C. Ghosh, S. Roy, and D. Cavalcanti, "Coexistence challenges for heterogeneous cognitive wireless networks in TV white spaces," *IEEE Wireless Commun.*, vol. 18, no. 4, pp. 22–31, Aug. 2011.

[9] F. Jasbi and D. K. C. So, "Hybrid overlay/underlay cognitive radio network with MC-CDMA," *IEEE Trans. Veh. Technol.*, vol. 65, no. 4, pp. 2038–2047, Apr. 2016.

[10] M. Pratibha, K. H. Li, and K. C. Teh, "Channel selection in multichannel cognitive radio systems employing RF energy harvesting," *IEEE Trans. Veh. Technol.*, vol. 65, no. 1, pp. 457–462, Jan. 2016.

[11] T. A. Tsiftsis, F. Foukalas, G. K. Karagiannidis, and T. Khattab, "On the higher order statistics of the channel capacity in dispersed spectrum cognitive radio systems over generalized fading channels," *IEEE Trans. Veh. Technol.*, vol. 65, no. 5, pp. 3818–3823, May 2016.

[12] E. Maratsolas, P. Koutsakis, and A. Lazaris, "Video activity-based traffic policing: A new paradigm," *IEEE Trans. Multimedia*, vol. 16, no. 5, pp. 1446–1459, Aug. 2014.

[13] H. Guo, K. Hu, and T. Xia, "Energy-efficient co-scheduling of receiving packets and decoding tasks on mobile video streaming terminals," in *Proc. IEEE Int. Conf. Multimedia Expo Workshops*, Jul. 2014, pp. 1–6.

[14] D. Kumar and G. Bhuvaneshwari, "Energy efficient packet scheduling to support real-time video streaming over Wi-MAX network," in *Proc. IEEE Int. Conf. Recent Trends Inf. Technol.*, Apr. 2012, pp. 108–113.

[15] Y. Xiao and M. van der Schaar, "Optimal foresighted packet scheduling and resource allocation for multi-user video transmission in 4G cellular networks," in *Proc. IEEE Int. Conf. Acoust., Speech Signal Process.*, May 2014, pp. 709–713.

[16] F. Li, P. Ren, and Q. Du, "Joint packet scheduling and subcarrier assignment for video communications over downlink OFDMA systems," *IEEE Trans. Veh. Technol.*, vol. 61, no. 6, pp. 2753–2767, Jul. 2012.

[17] P. Li, Y. Chang, N. Feng, and F. Yang, "A cross-layer algorithm of packet scheduling and resource allocation for multi-user wireless video transmission," *IEEE Trans. Consum. Electron.*, vol. 57, no. 3, pp. 1128–1134, Aug. 2011.

[18] Y. Li, A. Markopoulou, J. Apostolopoulos, and N. Bambos, "Content-aware playout and packet scheduling for video streaming over wireless links," *IEEE Trans. Multimedia*, vol. 10, no. 5, pp. 885–895, Aug. 2008.

[19] P. Pahalawatta, R. Berry, T. Pappas, and A. Katsaggelos, "Content-aware resource allocation and packet scheduling for video transmission over wireless networks," *IEEE J. Sel. Areas Commun.*, vol. 25, no. 4, pp. 749–759, May 2007.

[20] J. Hu, L. L. Yang, and L. Hanzo, "Maximum average service rate and optimal queue scheduling of delay-constrained hybrid cognitive radio in Nakagami fading channels," *IEEE Trans. Veh. Technol.*, vol. 62, no. 5, pp. 2220–2229, Jun. 2013.

[21] L. Zhou, R. Q. Hu, Y. Qian, and H. H. Chen, "Energy-spectrum efficiency tradeoff for video streaming over mobile ad hoc networks," *IEEE J. Sel. Areas Commun.*, vol. 31, no. 5, pp. 981–991, May 2013.

[22] L. Zhou, Z. Yang, Y. Wen, and J. J. P. C. Rodrigues, "Distributed wireless video scheduling with delayed control information," *IEEE Trans. Circuits Syst. Video Technol.*, vol. 24, no. 5, pp. 889–901, May 2014.

[23] N. Freris, C.-H. Hsu, J. Singh, and X. Zhu, "Distortion-aware scalable video streaming to multinetwork clients," *IEEE/ACM Trans. Netw.*, vol. 21, no. 2, pp. 469–481, Apr. 2013.
[24] M. Ismail, W. Zhuang, and S. Elhedhli, "Energy and content aware multihoming video transmission in heterogeneous networks," *IEEE Trans. Wireless Commun.*, vol. 12, no. 7, pp. 3600–3610, Jul. 2013.
[25] D. Jurca and P. Frossard, "Video packet selection and scheduling for multipath streaming," *IEEE Trans. Multimedia*, vol. 9, no. 3, pp. 629–641, Apr. 2007.
[26] M. Ismail and W. Zhuang, "Mobile terminal energy management for sustainable multi-homing video transmission," *IEEE Trans. Wireless Commun.*, vol. 13, no. 8, pp. 4616–4627, Aug. 2014.
[27] Z. He, S. Mao, and T. Jiang, "A survey of QoE-driven video streaming over cognitive radio networks," *IEEE Netw.*, vol. 29, no. 6, pp. 20–25, Nov. 2015.
[28] H. Kushwaha, Y. Xing, R. Chandramouli, and H. Heffes, "Reliable multimedia transmission over cognitive radio networks using fountain codes," *Proc. IEEE*, vol. 96, no. 1, pp. 155–165, Jan. 2008.
[29] H. T. Cheng and W. Zhuang, "Joint power-frequency-time resource allocation in clustered wireless mesh networks," *IEEE Netw.*, vol. 22, no. 1, pp. 45–51, Jan. 2008.
[30] M. K. Afzal, B. S. Kim, and S. W. Kim, "Efficient and reliable MPEG-4 multicast MAC protocol for wireless networks," *IEEE Trans. Veh. Tech.*, vol. 64, no. 3, pp. 1026–1035, Mar. 2015.
[31] Z. Pan, Y. Zhang, and S. Kwong, "Efficient motion and disparity estimation optimization for low complexity multiview video coding," *IEEE Trans. Broadcast.*, vol. 61, no. 2, pp. 166–176, Jun. 2015.
[32] Z. Pan, J. Lei, Y. Zhang, X. Sun, and S. Kwong, "Fast motion estimation based on content property for low-complexity H.265/HEVC encoder," *IEEE Trans. Broadcast.*, vol. 62, no. 3, pp. 675–684, Sep. 2016.
[33] F. Fu and M. van der Schaar, "Structural solutions for dynamic scheduling in wireless multimedia transmission," *IEEE Trans. Circuits Syst. Video Technol.*, vol. 22, no. 5, pp. 727–739, May 2012.
[34] M. Ismail, A. Abdrabou, and W. Zhuang, "Cooperative decentralized resource allocation in heterogeneous wireless access medium," *IEEE Trans. Wireless Commun.*, vol. 12, no. 2, pp. 714–724, Feb. 2013.

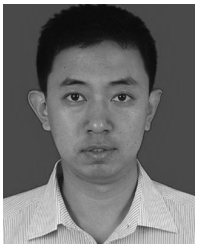

Lei Xu (M'16) received the Bachelor's, Master's, and Ph.D. degrees in communication and information systems from Nanjing University of Aeronautics and Astronautics, Nanjing, China, in 2006, 2009, and 2012, respectively.

He is currently an Associate Professor with the School of Computer Science and Engineering, Nanjing University of Science and Technology, Nanjing, China. His research interests include 5G wireless networks, network, analysis, Internet of things, satellite communication, and radar signal processing.

Arumugam Nallanathan (S'97–M'00–SM'05–F'17) is currently a Professor of wireless communications with the Department of Informatics, Kings College London (University of London), London, U.K. From 2011 and 2012, he was the Head of Graduate Studies with the School of Natural and Mathematical Sciences, Kings College London. From August 2000 to December 2007, he was an Assistant Professor with the Department of Electrical and Computer Engineering, National University of Singapore. He has published more than 300 technical papers in scientific journals and international conferences. His research interests include 5G wireless networks, Internet of things, and molecular communications.

Prof. Nallanathan received the Best Paper Award presented at the IEEE International Conference on Communications in 2016 and IEEE International Conference on Ultra-Wideband in 2007. He also received the IEEE Communications Society SPCE Outstanding Service Award in 2012 and the IEEE Communications Society RCC Outstanding Service Award in 2014. He is an IEEE Distinguished Lecturer. He was selected as a Thomson Reuters Highly Cited Researcher in 2016. He is an Editor for the IEEE TRANSACTIONS ON COMMUNICATIONS and the IEEE TRANSACTIONS ON VEHICULAR TECHNOLOGY. He was an Editor for the IEEE TRANSACTIONS ON WIRELESS COMMUNICATIONS (2006–2011), the IEEE WIRELESS COMMUNICATIONS LETTERS, and the IEEE SIGNAL PROCESSING LETTERS. He served as the Chair for the Signal Processing and Communication Electronics Technical Committee of IEEE Communications Society and Technical Program Chair and member of Technical Program Committees at numerous IEEE conferences.

Yuwang Yang received the B.S. degree from North-Western Polytechnical University, Xian, China, in 1988; the M.S. degree from the University of Science and Technology of China, Hefei, China, in 1991; and the Ph.D. degree from Nanjing University of Science and Technology (NUST), Nanjing, China, in 1996.

He is currently a Professor with the Department of Computer Science, NUST. His research interests include wireless sensor networks, industry control networks, and intelligent systems.